Development 134, 2903-2912 (2007) doi:10.1242/dev.007542

Evc is a positive mediator of Ihh-regulated bone growth that localises at the base of chondrocyte cilia

Victor L. Ruiz-Perez[1,2,*,†,‡], Helen J. Blair[1,*], M. Elena Rodriguez-Andres[2], Maria Jose Blanco[3], Amy Wilson[1], Yu-Ning Liu[1], Colin Miles[1], Heiko Peters[1] and Judith A. Goodship[1,‡]

EVC is a novel protein mutated in the human chondroectodermal dysplasia Ellis-van Creveld syndrome (EvC; OMIM: 225500). We have inactivated *Evc* in the mouse and show that *Evc*$^{-/-}$ mice develop an EvC-like syndrome, including short ribs, short limbs and dental abnormalities. *lacZ* driven by the *Evc* promoter revealed that *Evc* is expressed in the developing bones and the orofacial region. Antibodies developed against Evc locate the protein at the base of the primary cilium. The growth plate of *Evc*$^{-/-}$ mice shows delayed bone collar formation and advanced maturation of chondrocytes. Indian hedgehog (*Ihh*) is expressed normally in the growth plates of *Evc*$^{-/-}$ mice, but expression of the Ihh downstream genes *Ptch1* and *Gli1* was markedly decreased. Recent studies have shown that Smo localises to primary cilia and that Gli3 processing is defective in intraflagellar transport mutants. In vitro studies using *Evc*$^{-/-}$ cells demonstrate that the defect lies downstream of Smo. Chondrocyte cilia are present in *Evc*$^{-/-}$ mice and Gli3 processing appears normal by western blot analysis. We conclude that Evc is an intracellular component of the hedgehog signal transduction pathway that is required for normal transcriptional activation of *Ihh* target genes.

KEY WORDS: Evc, Ihh, Hedgehog signalling, Chondrocyte, Basal body, Gli3 processing

INTRODUCTION

The human disorder EvC is a chondroectodermal dysplasia comprising skeletal and craniofacial abnormalities in conjunction with dysplastic teeth and nails. The skeletal features are short ribs, short limbs, a defect of the lateral aspect of the proximal end of the tibia leading to genu valgum deformity, fusion of the hamate and capitate bones of the wrist and postaxial polydactyly. There is progressive shortening along the proximodistal axis of the limbs with zeugopod (radius-ulna/tibia-fibula) shortening being more marked than the shortening of the stylopod (humerus/femur), and in the autopod shortening of the distal phalanges being more marked than that of the proximal phalanges. Craniofacial abnormalities include multiple labiogingival frenulae, premature eruption of teeth including the presence of teeth at birth, small conical teeth and missing primary or permanent teeth. Approximately two thirds of affected individuals also have a cardiovascular malformation. Thirty of the 52 cases in Victor McKusick's description of the disorder in the Amish died within six months of birth, owing to the respiratory problems resulting from the small thorax and cardiovascular malformations (McKusick et al., 1964). Although medical management of both respiratory and cardiovascular problems has improved dramatically, there is still a significant mortality associated with this disorder.

By positional cloning we identified two genes, *EVC* and *EVC2*, which when mutated give rise to this condition (Ruiz-Perez et al., 2000; Ruiz-Perez et al., 2003). These genes are in close proximity, with a divergent orientation; the transcription starts sites are separated by 2,624 bp in human and by only 1,647 bp in mouse. *EVC* and *EVC2* encode novel proteins with putative transmembrane domains and regions of coiled-coiled structure, but on database interrogation show no similarity with any other proteins or motifs that give clues to their function. To determine which molecular pathways and developmental processes are perturbed in EvC, we developed anti-Evc antibodies to study subcellular localisation and generated a mouse model. As the majority of mutations identified in *EVC* (Tompson et al., 2007) are predicted to cause loss of function, we ablated gene function in the mouse.

The major features of EvC are shortening of the long bones and ribs. Although many signalling molecules and pathways are involved in skeletal development, Indian hedgehog (Ihh) is the master regulator (Kronenberg, 2003). In the growth plates of long bones, Ihh is secreted by the prehypertrophic chondrocytes, generating a gradient of signal that coordinates chondrocyte differentiation, chondrocyte proliferation and perichondrial development (Kronenberg, 2003). Previous work involving chimeras and knockout mice has shown that Ihh regulates chondrocyte differentiation by stimulating the synthesis of parathyroid hormone-like peptide (Pthrp; also known as Pthlh – Mouse Genome Informatics) in the periarticular region (Chung et al., 1998; St-Jacques et al., 1999; Vortkamp et al., 1996). Pthrp, which is also a paracrine signalling molecule, diffuses back towards the centre of the developing bones and acts on the parathyroid hormone (Pth)/Pthrp receptor (PPR; also known as Pthr1– Mouse Genome Informatics) to prevent proliferative columnar chondrocytes differentiating into postmitotic hypertrophic cells (Karaplis et al., 1998; Lanske et al., 1996; Weir et al., 1996). By doing this, Pthrp suppresses Ihh expression in early hypertrophic cells and an Ihh-Pthrp negative feedback loop is established to regulate the distance from the joint at which chondrocytes leave the proliferative pool and undergo hypertrophy (Chung et al., 1998; Vortkamp et al., 1996). Accordingly, Ihh-depleted mice have abnormal growth plates with undetectable levels of Pthrp expression in which chondrocytes undergo hypertrophy closer to the ends of

[1]Institute of Human Genetics, Newcastle University, Central Parkway, Newcastle upon Tyne NE1 3BZ, UK. [2]Centro de Investigaciones Biológicas, Consejo Superior de Investigaciones Científicas, Ramiro de Maeztu 9, 28040 Madrid, Spain. [3]Department of Human Anatomy and Embryology, Faculty of Medicine, Universidad Complutense de Madrid, 28040 Madrid, Spain.

*These authors contributed equally to this work
[†]Present address: Instituto de Investigaciones Biomédicas, Consejo Superior de Investigaciones Científicas, Arturo Duperier 4, 28029 Madrid, Spain
[‡]Authors for correspondence (e-mails: vlruiz@iib.uam.es; j.a.goodship@ncl.ac.uk)

Accepted 7 June 2007

bones and lack the characteristic stacked columns of proliferating chondrocytes. In addition, Ihh mutants display Pthrp-independent defects, including dramatic reduction in chondrocyte proliferation and failure of cortical bone formation (Razzaque et al., 2005; St-Jacques et al., 1999).

In vertebrates, there are three hedgehog (Hh) signalling molecules [sonic hedgehog (Shh), Ihh and desert hedgehog (Dhh)] whose effects are mediated by three different Gli transcription factors (Gli1-3). The essence of Hh signalling is that binding of Hh molecules to their receptor, patched (Ptch), releases inhibition of smoothened (Smo), the activator of the Hh pathway. Smo prevents phosphorylation and cleavage of full-length Gli3 (Gli3-190) to the transcriptional repressor Gli3R (Gli3-83) and promotes Gli transcriptional activation (Hooper and Scott, 2005).

It has been shown that vertebrate Hh signalling is mediated through primary cilia. Cilia are essential for Shh-mediated patterning in early limb bud and neural tube development (Huangfu et al., 2003; Liu et al., 2005). Important components of the pathway, suppressor of fused (Sufu) and the Gli proteins, localise to primary cilia and Smo translocates to cilia upon pathway activation (Corbit et al., 2005; Haycraft et al., 2005). The recent generation of a *Prx1Cre* (also known as *Prrx1-cre*) conditional allele of *Ift88* has enabled study of cilia-dependent processes in mesenchyme-derived tissues of the limb and confirms, as anticipated, that cilia are also required for Ihh signalling (Haycraft et al., 2007). In mutants with disrupted anterograde or retrograde intraflagellar transport, Gli3 processing is abnormal with an increase in full-length Gli3 and decreased levels of Gli3R (Haycraft et al., 2005; Huangfu and Anderson, 2005; Liu et al., 2005; May et al., 2005). Despite the increase in full-length Gli3 in intraflagellar transport (IFT) mutants, all have low expression levels of the readouts of the pathway, *Gli1* and *Ptch1* (Huangfu et al., 2003; Liu et al., 2005), proving that inhibition of Gli processing is not sufficient to produce transcriptional activation and that additional IFT-dependent events are required to promote Gli activator functioning.

Here we report that Evc localises at the base of primary cilia and demonstrate that defective transduction of Ihh signalling underlies the skeletal phenotype associated with Evc mutation. Our findings show that Evc acts as a positive mediator of Hh signalling downstream of Smo, but that it is not essential for Gli processing.

MATERIALS AND METHODS

Evc$^{-/-}$ mouse generation and genotyping

The *Evc* targeting vector was engineered to simultaneously create an in-frame fusion of β-galactosidase (β-gal) to the first amino acid of Evc and ablate gene function by deleting the downstream remaining *Evc* exon 1 sequence (Fig. 1A). The 5′ and 3′ DNA arms of homologous sequence were isolated from a 129/SvJ BAC clone (Genome Systems) and the *lacZ* cassette from plasmid pSDKLacZpA. The linearised targeting vector was electroporated into AB1 ES cells and homologous recombinant clones injected into C57BL/6 blastocysts. Male chimeras were bred to C57BL/6 female mice and germline transmission confirmed by PCR and Southern blot (Fig. 1B). Mice were PCR genotyped by simultaneous amplification of *Evc* exon 1 (170 bp) and *lacZ* (475 bp) (Fig. 1C). Absence of *Evc* transcript in *Evc*$^{-/-}$ mice was confirmed by RT-PCR (Fig. 1D). Given the close proximity of *Evc2* to *Evc*, we compared *Evc2* expression in chondrocytes from two E17.5 mutant embryos with two wild-type littermates by quantitative PCR and found similar expression (data not shown). As *Evc* 3′ untranslated exons overlap with *Crmp1* 3′ exons, we

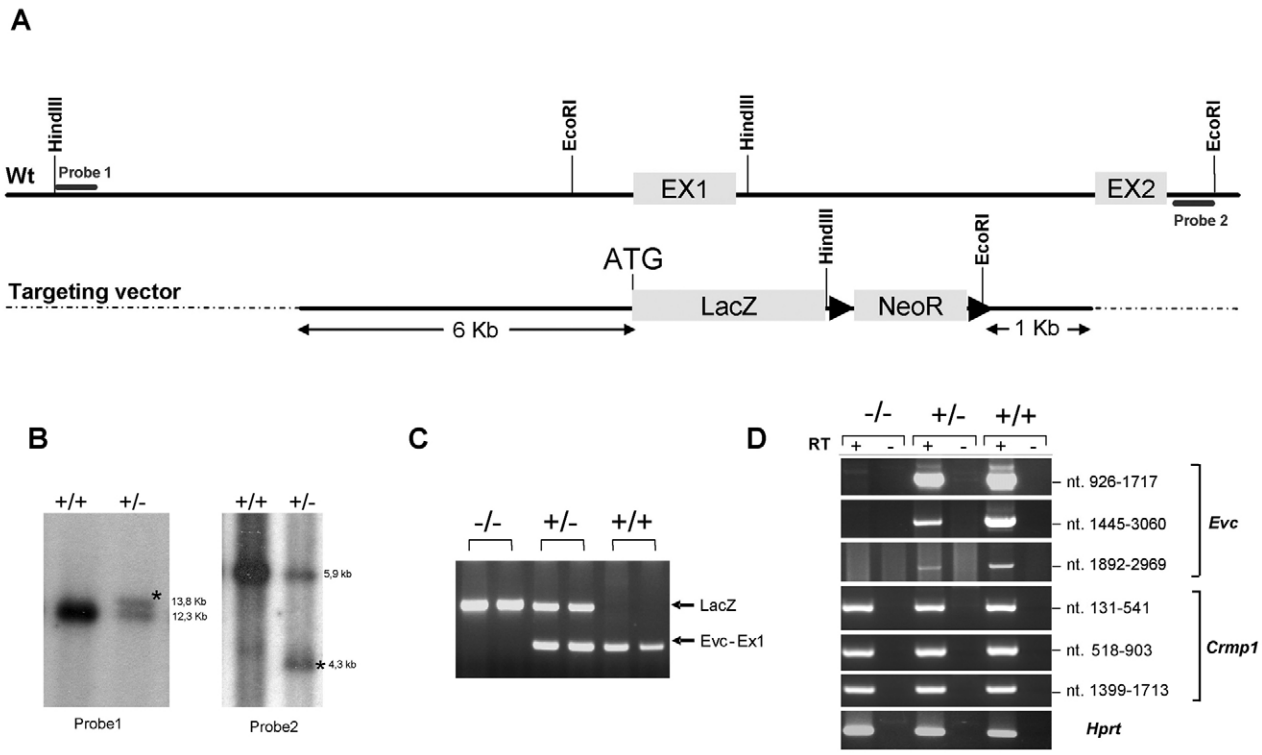

Fig. 1. Generation of *Evc*$^{-/-}$ mice. (**A**) Wild-type *Evc* allele and the targeting vector. The length of homologous sequence flanking the *lacZ* and neomycin resistance cassettes in the targeting vector is indicated; the two loxP sites are shown as triangles. (**B**) Southern blot analysis confirming homologous recombination at the *Evc* locus. DNA from wild-type and *Evc*$^{+/-}$ mice was digested with *Hin*dIII (left) or *Eco*RI (right) and hybridised, respectively, with probes 1 and 2 (see A). Asterisks designate hybridisation signals corresponding to the targeted allele. (**C**) PCR products from tail-tip genotyping. (**D**) RT-PCR showing total absence of *Evc* transcript in *Evc*$^{-/-}$ mice and unaffected transcription of *Crmp1*. Three different primer pairs were used to amplify *Evc* cDNA (NM_021292) downstream of exon1 and *Crmp1* cDNA (NM_007765). *Hprt* was used as a control.

checked that removal of the *Evc* transcript did not affect transcription of *Crmp1* (Fig. 1D). Mice were maintained by crossing $Evc^{+/-}$ males to F1 females from C57Bl/6×129 crosses.

Antibody production

Amino acids 459-999 of the mouse Evc protein (GenBank CAB76567) were expressed with a 6×His tag in *E. coli* and purified by Ni^{2+} chelation chromatography (Novagen). The protein (150 μg) was used to immunise sheep (Diagnostic Scotland). Total IgGs were prepared from final serum (Protein G HiTrap, Amersham) and anti-Evc antibodies purified by affinity to the antigen conjugated to AminoLink Coupling Gel (Pierce).

Immunofluorescent staining

Tissue was frozen in OCT and cryosections (10 μm) dried onto charged slides. mIMCD3 cells were cultured using standard conditions. Tissue sections and cells were fixed in 4% (w/v) paraformaldehyde (PFA) in PBS at 4°C. Primary antibodies were: sheep polyclonal anti-Evc (5 μg/ml); mouse monoclonal anti-γ-tubulin (1:800, GTU-88, Sigma) and anti-acetylated tubulin (1:2000, 6-11B-1, Sigma). Secondary antibodies were: donkey anti-sheep Alexa Fluor 594 (Molecular Probes) and goat anti-mouse FITC (Sigma). Samples were mounted in Vectashield with DAPI (Vector) and images captured on an Axioplan 2 fluorescence microscope (Zeiss).

Whole-mount X-Gal staining, skeletal preparations and X-ray analysis

$Evc^{+/-}$, $Evc^{-/-}$ and wild-type control embryos were stained for β-gal activity with X-Gal as previously described (Hogan et al., 1994; Schatz et al., 2005). E15.5 embryo heads and newborn hindlimbs were stained with X-Gal and embedded in a gelatine/albumin mix for vibratome sectioning. Sections (100 μm) were mounted in 50% (v/v) glycerol in PBS for photographing. Skeletal preparations of P6 mice were conducted as previously described (Kessel and Gruss, 1991). Digital radiographs of euthanised P1 and P18 mice were collected at X-ray exposures of 30 kV for 5 seconds and 45 kV for 10 seconds, respectively. Bones measurements were compared by ANOVA.

Histology and BrdU analysis

Embryo limbs were fixed in 4% PFA in PBS and paraffin embedded. P16 limbs were decalcified in 4% formaldehyde:nitric acid:H_2O (1:1:8) for a week prior to embedding. Sections (7 μm) were stained with Haematoxylin-Eosin or by trichromic staining (0.13% Light Green SF Yellowish, 0.16% Orange G, 0.2% fuchsin acid). Standard von-Kossa method was used for detection of mineralisation. E17.5 pregnant females were sacrificed 5 hours after receiving an intraperitoneal injection of BrdU cell proliferation labelling reagent (GE Healthcare). Proliferating cells were detected on 7 μm paraffin sections by immunocytochemistry (BrdU Staining Kit, Zymed). BrdU-positive and BrdU-negative nuclei were counted in columnar chondrocytes of $Evc^{-/-}$ and wild-type mice (12 and seven sections, respectively). The percentage BrdU-positive cells was calculated for each section and data compared by ANOVA.

In situ hybridisation

Hindlimbs from E16.5 littermates were fixed overnight in 4% PFA in PBS, decalcified in 14% (w/v) EDTA in PBS and paraffin embedded. Sections (10 μm) were hybridised using 2×10^7 cpm/ml ^{35}S-labelled antisense riboprobes, except for *Col2a1* and *Col10a1*, which were digoxigenin labelled (Roche). Hybridisation steps were as in Lescher et al. (Lescher et al., 1998). After stringency washes, dehydrated sections were coated with nuclear emulsion (K5, Ilford) and exposed for 2-4 weeks at 4°C. Signal was developed in Kodak D-19 developer and fixer and sections counterstained with nuclear Fast Red. Hybridisation probes were obtained by request, except for *Gli1* (AB025922) and mouse *PPR* (NM_011199), which were RT-PCR amplified. Bright-field images were obtained on a Nikon DS-5L1 digital camera and dark-fields produced in Photoshop (Adobe).

Purmorphamine treatment of cells and quantification of target genes

Mouse embryonic fibroblasts (MEFs) were established from $Evc^{-/-}$ and control E14.5 embryos (Todaro and Green, 1963). Chondrocytes were isolated from tibial epiphysial cartilage dissected from two E17.5 $Evc^{-/-}$ and two $Evc^{+/+}$ littermates as described (Shingleton et al., 2000) with the following modifications to enzyme incubation times: hyaluronidase, 5 minutes; trypsin, 10 minutes; collagenase, 5 hours. Chondrocytes were incubated in DMEM containing 10% fetal calf serum at 2×10^6 cells in 6-well plates for a maximum of 7 days following dissection. For Hh pathway induction experiments, 1×10^5 cells were grown overnight in 12-well plates and treated for 72 hours with either 2 μM purmorphamine (10 mM stock in DMSO, Calbiochem) or DMSO alone. Simultaneous RT-PCR amplification of *Ptch1* (nt 1944-2303; NM_008957) and *Hprt* (nt 108-294; NM_013556) in MEF cDNA was performed for 22 cycles under standard PCR conditions. Assays were carried out twice on cultures derived from three $Evc^{-/-}$, two $Evc^{+/+}$ and one $Evc^{+/-}$ embryo. Ratios of *Ptch1* to *Hprt* band intensity were determined for each culture before and after treatment and compared by ANOVA. For the quantitative PCR experiments, chondrocyte cDNA samples were loaded onto Taqman Low Density Array (TLDA) microfluidic cards (ABI, Forster City, CA). The following primers and probes were used: *Gli1* (ABI assay ID. Mm00494645_m1), *Ptch1* (ABI assay ID. Mm00436026_m1), *Evc* (ABI assay ID. Mm00469587_m1), *Evc2* (ABI assay ID. Mm00507589_m1) and β-actin (*Actb*; ABI assay ID. Mm00607939_s1). Relative quantification of genes was performed using the ABI Prism 7900HT Sequence Detection System and expressed as arbitrary units as determined by $2^{-(\text{Ct gene}-\text{Ct β-actin})}$.

Gli3 western blot

Protein lysate from E14.5 limbs was prepared in RIPA buffer supplemented with one Mini Complete Protease Inhibitor tablet (Roche) and 0.1M PMSF. Total protein was electrophoresed on 7.5% SDS-PAGE gels and transferred to Hybond-C membrane (Amersham). Gli3 was detected using rabbit anti-Gli3 (1:200, a gift of B. Wang, Cornell University, NY) followed by goat anti-rabbit peroxidase (1:5000, Jackson ImmunoResearch) and SuperSignal West Dura Extended Duration Substrate (Pierce). Protein loading was assessed using rabbit anti-β-catenin (BD Biosciences).

RESULTS

Evc localises at the base of chondrocyte cilia but is not required for ciliogenesis

Using the Evc antibodies and γ-tubulin and acetylated tubulin as markers of centrioles and cilia axoneme, respectively, we found that Evc localises at the distal end of the maternal centriole (the basal body), at the base of the axoneme (Fig. 2A,B), suggestive of localisation to the transition zone. Specificity of the Evc immunostaining was demonstrated by absence of signal in chondrocytes from $Evc^{-/-}$ mice (Fig. 2C). Cilia were present in $Evc^{-/-}$ chondrocytes, demonstrating that Evc is not essential for ciliogenesis (Fig. 2C).

Evc is expressed in the developing skeleton and the orofacial region

During construction of the *Evc* targeting vector, we inserted a *lacZ* reporter cassette directly under control of the *Evc* promoter to determine the *Evc* spatiotemporal expression pattern during development. By whole-mount X-Gal staining of $Evc^{+/-}$ mouse embryos, we first observed *lacZ* expression at E11.5 in the orofacial region in the lateral nasal process, maxillary and mandibular processes (Fig. 3A-D), followed at E12.5 by expression in the mesenchymal condensations of the skeletal system at the time they initiate chondrocyte differentiation (Fig. 3C). At E15.5, vibratome sectioning of the orofacial region demonstrated β-gal activity in the cartilages of the nasal septum and nasal capsule and those enclosing the Jacobson organ (Fig. 3E). Strong β-gal activity was also evident in the upper and lower lip mesenchyme and in the mesenchyme outlining the growing bones of the maxilla and mandible (Fig. 3H). By E15.5, *lacZ* expression was general to all the cartilaginous components of the skeleton, including the chondrocranium, the vertebrae, the rib cage

and the axial skeleton (Fig. 3F,G). In the developmentally more advanced elements of the axial skeleton, *lacZ* expression was narrowed to the chondrocytes of the epiphysis and the perichondrium and absent in the central bone metaphyses. However, in the phalanges in which chondrocytes have not yet undergone hypertrophy, the entire element was *lacZ*-positive. In order to determine which type of chondrocytes express *Evc*, we studied newborn skeletal growth plates in which chondrocyte layers are more easily distinguishable. Vibratome sectioning of stained newborn skeletal growth plates showed β-gal activity in the perichondrium and in resting and proliferating chondrocytes (Fig. 3M,N), but no activity in the prehypertrophic and hypertrophic chondrocytes. Finally, we observed β-gal activity in the cranial sutures, suggesting a role in both endochondral and intramembranous ossification. We detected *lacZ* expression in nails (Fig. 3L), the dermal papilla of the vibrissae (Fig. 3J) and in the mesenchyme surrounding the developing tooth buds (Fig. 3I), in keeping with the ectodermal phenotype seen in EvC patients.

Evc$^{-/-}$ mice have an Ellis-van Creveld syndrome-like chondrodysplasia

Evc$^{+/-}$ mice have no discernable defects. Offspring from heterozygous *Evc*$^{+/-}$ crosses were genotyped at E18.5 just prior to birth and there was no deviation from mendelian ratios by χ^2 tests and thus no prenatal loss of *Evc*$^{-/-}$ embryos was detected. However, approximately half of the *Evc*$^{-/-}$ offspring were missing 2 days after birth. These neonatal losses are unlikely to be due to cardiovascular malformation because no overt cardiovascular malformations were observed on histological examination of 14 *Evc*$^{-/-}$ mice (eight at E14.5, one at E15.5, four at E18 and one newborn) (results not shown). Surviving *Evc*$^{-/-}$ mutants were unable to feed on a normal diet, but were able to survive to adulthood when supplied with soft, well-hydrated food; they did not breed. The phenotype of *Evc*$^{-/-}$ mice recapitulates the human disorder with short ribs, short limbs and dental anomalies, although they do not have polydactyly (Fig. 4A,B). Preliminary examination of the teeth revealed variability in the abnormalities of the incisors, including absence of the upper incisors and a single upper incisor. We frequently observed a smaller first molar, in comparison with wild-type dentition (Fig. 4C).

We focussed on analysis of the skeletal abnormalities and commenced by studying radiographs and skeleton preparations. At birth, there was no difference between the head-to-tail length of wild-type and mutant mice, but the rib cage was narrow and the radius, ulna, femur and tibia were shorter in the mutant mice (see Table S1 in the supplementary material). At P18, radiographs revealed that the mutant mice are smaller than littermates, that the rib cage is small and that shortening of the radius, ulna and tibia is more pronounced than for the humerus and femur, indicating the same pattern of bone shortening in the mouse mutant as in patients with EvC (Fig. 4A). These observations were confirmed by measurements taken from the radiographs, with decreased radius/humerus (P=0.00065), tibia/femur (P=0.0045) and rib cage/body length (P=0.00853) ratios at P18 (see Table S1 in the supplementary material). Alcian Blue-Alizarin Red skeletal staining also demonstrated this pattern of limb shortening and in addition showed an irregular margin between bone and cartilage in the basiocciput and costochondral junctions (Fig. 4B), as well as premature mineralisation of some of the pedicles between the vertebral bodies and vertebral laminae (Fig. 4B, arrows).

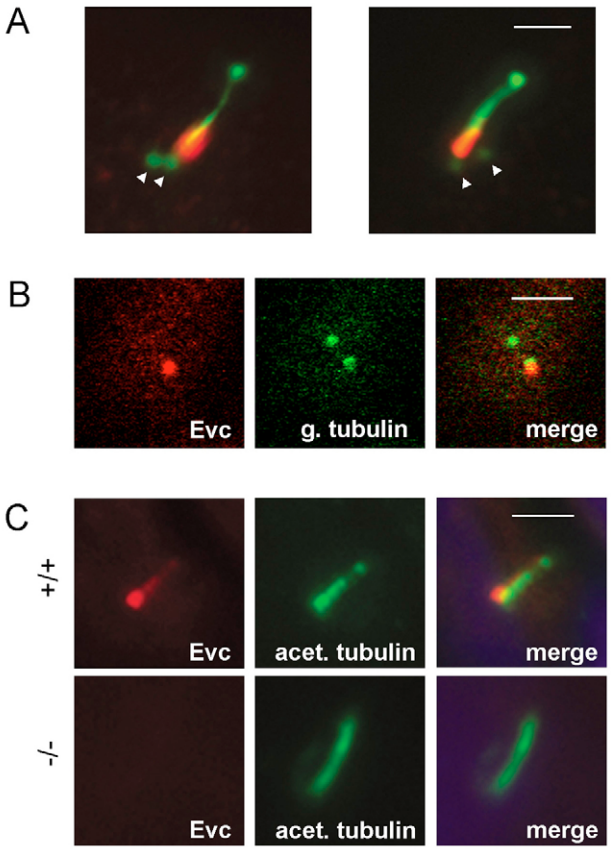

Fig. 2. Evc localises to the basal body and is not required for ciliogenesis. (**A**) Acetylated tubulin and γ-tubulin immunofluorescence (green) distinguish the ciliary axoneme and the two centrioles, respectively, in mIMCD3 cells. Anti-Evc (red) reveals Evc to be localised at the base of the cilium. Arrowheads, centrioles. (**B**) γ-tubulin (green) and Evc (red) immunofluorescence show that Evc signal overlaps with one of the two centrioles. (**C**) In situ Evc immunostaining of wild-type and Evc$^{-/-}$ chondrocytes of P0 proximal tibia demonstrate Evc localisation, the presence of cilia in the mutant and the specificity of the antibody. Scale bar: 2 μm.

Abnormal growth plate development in the long bones of *Evc*$^{-/-}$ mice

Histological analysis of embryonic growth plates revealed shorter proliferative and hypertrophic chondrocyte layers in the epiphyses of the long bones with hypertrophy of chondrocytes occurring closer to the articular region than in the wild-type controls. Chondrocytes in the proliferative zone in *Evc*$^{-/-}$ mice had the characteristic flattened shape (Fig. 5A). We consistently observed an abnormality in the shape of the upper end of the tibia (Fig. 5A,C), comparable to that seen in EvC patients. We studied mineralisation by von-Kossa staining and detected delayed formation of the periosteum adjacent to the prehypertrophic and hypertrophic chondrocytes (Fig. 5B, red arrows). Similarly, trichromic staining in older mice demonstrated delayed formation of the secondary ossification centres (Fig. 5C).

Ihh signalling is diminished in *Evc*$^{-/-}$ mice, although Gli3 processing appears to be normal

The phenotypic observations of epiphyseal shortening due to chondrocytes hypertrophying nearer to the articular region, defective perichondrium to periosteum induction and mineralisation of

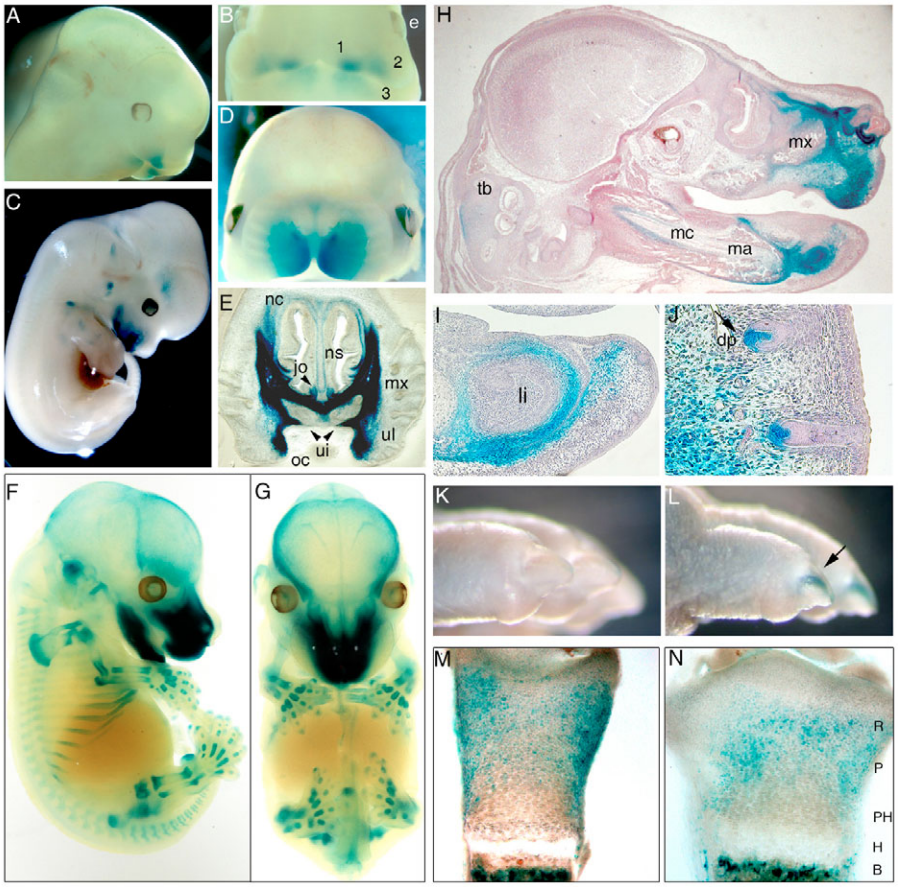

Fig. 3. *Evc* expression pattern. β-gal activity at E11.5 (**A**,**B**), E12.5 (**C**), E13.5 (**D**), E15.5 (**E-J**) and in newborn (**K-N**) mice demonstrating expression in the mouth and tooth-forming areas and in the developing skeleton. The ossified centres of the long bones are not β-gal-positive. E is a coronal vibratome section of the head of an embryo. H,I,J are sagittal paraffin sections of the head, lower jaw and vibrissae. (K,L) Absence of endogenous β-gal activity in control (K) and expression of *lacZ* in the proximal nail bed in $Evc^{-/-}$ (L, arrow) mice. (M,N) Vibratome sections showing growth plates of distal (M) and proximal (N) tibia of newborn mice. The blue signal in the bone marrow is background, as it was also detected in equivalent wild-type sections. *Evc* expression has the same distribution in heterozygotes and mutants from E12.5 to birth. All images relate to $Evc^{+/-}$ embryos with the exception of newborn mice (L-N), which were $Evc^{-/-}$, and K which was wild-type. 1, lateral nasal process; 2, maxillary process; 3, mandibular process; e, eye; ns, nasal septum; nc, nasal capsule; jo, Jacobson´s organ; ul, upper lip; oc, oral cavity; ui, upper incisor; mx, maxilla; ma, mandible; mc, Meckel's cartilage; tb, temporal bone; li, lower incisor; dp, dermal papillae. Growth plate chondrocytes labelling: R, resting; P, proliferative; PH, prehypertrophic; H, hypertrophic; B, bone.

synchondroses are all factors compatible with impaired Ihh signalling in mice (Hilton et al., 2005; Koziel et al., 2005; Razzaque et al., 2005; St-Jacques et al., 1999). In addition, Evc localises to the base of cilia, structures that mediate Hh signalling (Huangfu and Anderson, 2005). We therefore decided to determine whether defective Hh signalling underlies the $Evc^{-/-}$ skeletal phenotype and assessed expression of Ihh signalling molecules in the growth plates of $Evc^{-/-}$ mice by radioactive in situ hybridisation. We found *Ihh* expression in prehypertrophic chondrocytes of $Evc^{-/-}$ mice to be normal. However, expression of the Ihh downstream targets *Ptch1* and *Gli1* was drastically reduced in the adjacent perichondrium and proliferating chondrocytes, providing evidence of defective Ihh signalling (Fig. 6A). To corroborate this, we derived mouse embryonic fibroblasts (MEFs) from $Evc^{-/-}$ and control littermates and assessed induction of *Ptch1* expression under exogenous stimulation of the pathway with purmorphamine (Sinha and Chen, 2006; Wu et al., 2004). RT-PCR results from MEF cultures showed that the *Ptch1* response of purmorphamine-treated $Evc^{-/-}$ MEFs was diminished compared with wild-type MEFs (Fig. 6B). The mean ratio of *Ptch1*:*Hprt* expression was significantly different between $Evc^{-/-}$ and wild-type fibroblast cultures grown in the presence of purmorphamine (ANOVA, P=0.003). In addition, we assessed *Ptch1* and *Gli1* transcript levels following purmorphamine treatment by quantitative RT-PCR in chondrocytes derived from $Evc^{-/-}$ and wild-type littermates. The *Ptch1* (Fig. 6C) and *Gli1* (Fig. 6D) response of $Evc^{-/-}$ purmorphamine-treated chondrocytes was greatly diminished compared with control cells. Since purmorphamine is a Hh agonist that targets Smo, these studies confirm abnormal Hh signalling in *Evc* mutants and demonstrate an intracellular defect downstream of Smo.

The *Evc* expression pattern we observed in the growth plate (Fig. 3M,N) is similar to that of Ihh target genes. To investigate whether *Evc* could be under Ihh regulation, we assessed *Evc* expression in wild-type chondrocytes by quantitative PCR. Exogenous stimulation of the pathway with purmorphamine did not alter *Evc* transcript levels (data not shown).

Cilia and IFT proteins have been shown to be required for proteolytic processing of Gli3. Gli3R is dramatically decreased and full-length Gli3 dramatically increased in IFT mutant embryos at E9.5-11.5 (Haycraft et al., 2005; Liu et al., 2005). Western blot analysis of protein extracted from E10.5 $Evc^{-/-}$ and control embryos revealed normal levels of both full-length Gli3 and Gli3R (results not shown). However, as there is no detectable β-gal activity in $Evc^{+/-}$ or $Evc^{-/-}$ embryos at this point in development, we tested whether Evc is required for Gli3 processing in limb extracts from E14.5 embryos. Levels of Gli3, particularly full-length Gli3, have previously been shown to be very low in the E14.5 limb (Hilton et al., 2005). We did not observe a change in the levels of either full-length Gli3 or Gli3R in E14.5 $Evc^{-/-}$ limb extracts when compared with littermate controls (Fig. 6E).

Proliferation is normal but differentiation from columnar to hypertrophic chondrocytes occurs prematurely in $Evc^{-/-}$ mice

One of the features of *Ihh*-knockout mice is a striking proliferation deficiency known to be caused by the increase in Gli3 repression (Hilton et al., 2005; Koziel et al., 2005). To test whether proliferation is affected in *Evc* mutants, we undertook in vivo BrdU labelling experiments followed by immunohistochemistry. No significant difference was observed in the percentage of BrdU-positive

chondrocytes between *Evc*$^{-/-}$ and wild-type mice in the proximal tibia at E17.5 (Fig. 7A). As proliferation and apoptosis (data not shown) do not seem to be affected, we hypothesised that the growth plate shortening in *Evc*$^{-/-}$ mice is likely to be due to premature chondrocyte differentiation.

To assess differentiation, we first analyzed expression of *Col2a1* and *Col10a1* and observed that *Evc*$^{-/-}$ chondrocytes undergo normal endochondral ossification from *Col2a1*-positive resting-proliferating chondrocytes to *Col10a1*-expressing hypertrophic chondrocytes (Fig. 7B). Since Pthrp is the principal molecule controlling chondrocyte maturation (Kronenberg, 2003), we went on to study Pthrp signalling and found that *Pthrp* expression in articular chondrocytes, which is normally maintained by Ihh signalling, was decreased (Fig. 7B). We observed normal expression of the Pth/Pthrp receptor, *PPR*, in the prehypertrophic zone, but expression in the osteoprogenitor cells of the perichondrium (Naski et al., 1998) (Fig. 7B, arrows) was reduced in the *Evc*$^{-/-}$ growth plate (Fig. 7B), in keeping with the mineralisation defect in the perichondrium evidenced by the von-Kossa staining.

To further clarify whether *Evc*$^{-/-}$ growth plate shortening is due to premature differentiation from distal to columnar chondrocytes, or from columnar to hypertrophic chondrocytes, or both, we supplemented the histological analysis by studying *Fgfr1* expression as a marker of distal and hypertrophic chondrocytes and *Fgfr3* expression as a marker of columnar and early hypertrophic cells. The hybridisation results showed that there was no shortening of the distal *Fgfr1* expression domain in *Evc*$^{-/-}$ mice, but marked shortening of the zone expressing *Fgfr3* (Fig. 7C), from which we conclude that differentiation from distal to columnar chondrocyte, which is influenced by Gli3R (Koziel et al., 2005), is proceeding normally and hypertrophic differentiation is occurring prematurely.

DISCUSSION

In this study, we demonstrate that defective Ihh signalling underlies the skeletal features in mice lacking Evc. By in situ hybridisation, we have shown that there is decreased expression of the Ihh targets *Gli1*, *Ptch1* and *Pthrp* in the growth plates of *Evc*$^{-/-}$ mice, although expression of *Ihh* itself is normal. Reduced target gene expression could result from defective production or diffusion of the signal or from defective cell response upon Ihh arrival. *lacZ* expression analysis of the growth plate helped to distinguish between these possibilities as X-Gal predominantly stained proliferating and distal chondrocytes and the perichondrium, cells that respond to Ihh signal, but left the region of Ihh-secreting prehypertrophic cells unstained. From this we deduced that Evc was likely to be involved in transduction of the response to Ihh signal. Confirmation came from the in vitro experiments in which we supplemented MEFs and chondrocytes with the Smo agonist purmorphamine. These experiments verified, by an independent method, that *Evc*$^{-/-}$ cells exhibit diminished upregulation of *Ptch1* and *Gli1* in response to signal, and demonstrated that the defect lies downstream of Smo. Smo blocks proteolytic processing of Gli3 and also plays a role in conferring activator status to full-length Gli3. Western blot analysis and indirect evidence (normal proliferation and normal differentiation from distal to columnar chondrocytes) demonstrate that Gli3R is not increased, indicating that Gli3 processing occurs normally in Evc-depleted mice.

The *Evc*$^{-/-}$ phenotype is less severe than that of *Ihh*$^{-/-}$ because Gli3R is not increased

The phenotype in *Ihh*$^{-/-}$ mice is far more severe than that in mice lacking Evc. This is because the absence of Ihh is associated not only with removal of Gli activator functions, but also with increased Gli3 repression, with some aspects of the *Ihh*$^{-/-}$

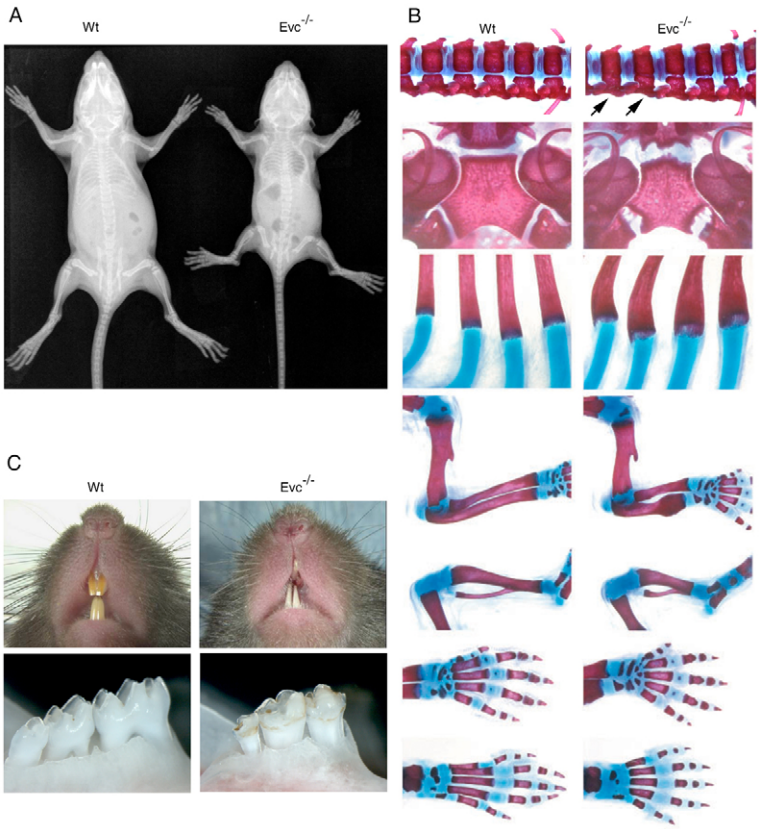

Fig. 4. Phenotype of *Evc*$^{-/-}$ mice. (**A**) Radiographs at P18. (**B**) Skeletal staining of the vertebral column, basiocciput, ribs, forelimb, hindlimb, forepaw and hindpaw of P6 mice. There is premature mineralisation across vertebral synchondroses in the mutant (arrows), an irregular margin between bone and cartilage in the basiocciput and costochondral junctions, shortening of the radius and ulna, tibia, metacarpals and metatarsals and a modelling defect at the distal ulna. (**C**) Mutants (upper panels) showed small dysplastic incisors and (lower panels) conical lower molars, size reduction of the first molar and an enamel defect.

phenotype resulting from decreased Gli activation and some being due to increased Gli3R repression. Analysis of *Ihh*$^{-/-}$,*Gli3*$^{-/-}$ double knockout mice, in which Gli3 repression is abolished in an *Ihh*$^{-/-}$ background, has shown which features of the *Ihh*$^{-/-}$ phenotype result from elevated Gli3R (Hilton et al., 2005; Koziel et al., 2005). The proliferation deficiency in the growth plate of *Ihh*$^{-/-}$ mice is fully rescued in the double knockouts and is therefore attributable to increased Gli3 repression. Gli3R levels are normal in *Evc*$^{-/-}$ mice and, consistent with this, chondrocyte proliferation in *Evc*$^{-/-}$ mice is normal. By contrast, in the growth plates of the *Ihh*$^{-/-}$,*Gli3*$^{-/-}$ mice, there is no *Gli1* expression and there is only partial recovery of the reduced levels of *Pthrp* and

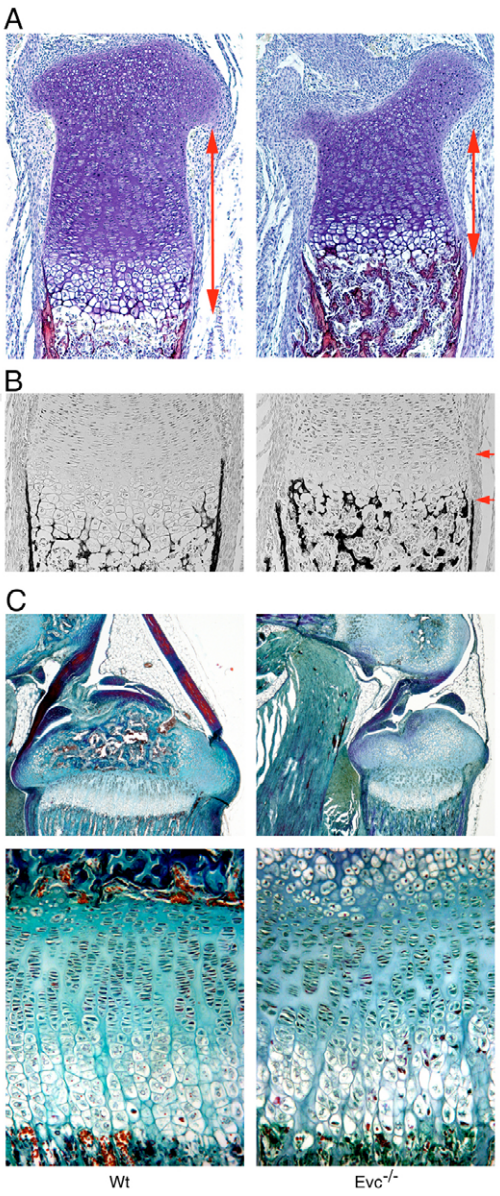

Fig. 5. The growth plate in *Evc*$^{-/-}$ mice. In all panels, the wild type is shown on the left, *Evc*$^{-/-}$ mutant on the right. (**A**) Haematoxylin-Eosin staining of the upper end of the tibia of E17.5 embryos. The proliferative and hypertrophic zones are indicated by arrows. The mutant epiphysis lacks the normal convex shape. (**B**) von-Kossa staining of the upper end of tibia from E17.5 embryos. Arrows indicate absent perichondrial mineralisation. (**C**) Top, trichromic staining of the knee joint at P16 showing delay of secondary ossification and a defect in the shape of the tibial epiphysis. Below, magnification of the P16 growth plates from panels above, showing disorganised growth plate structure and fewer cells in the columns of proliferative chondrocytes.

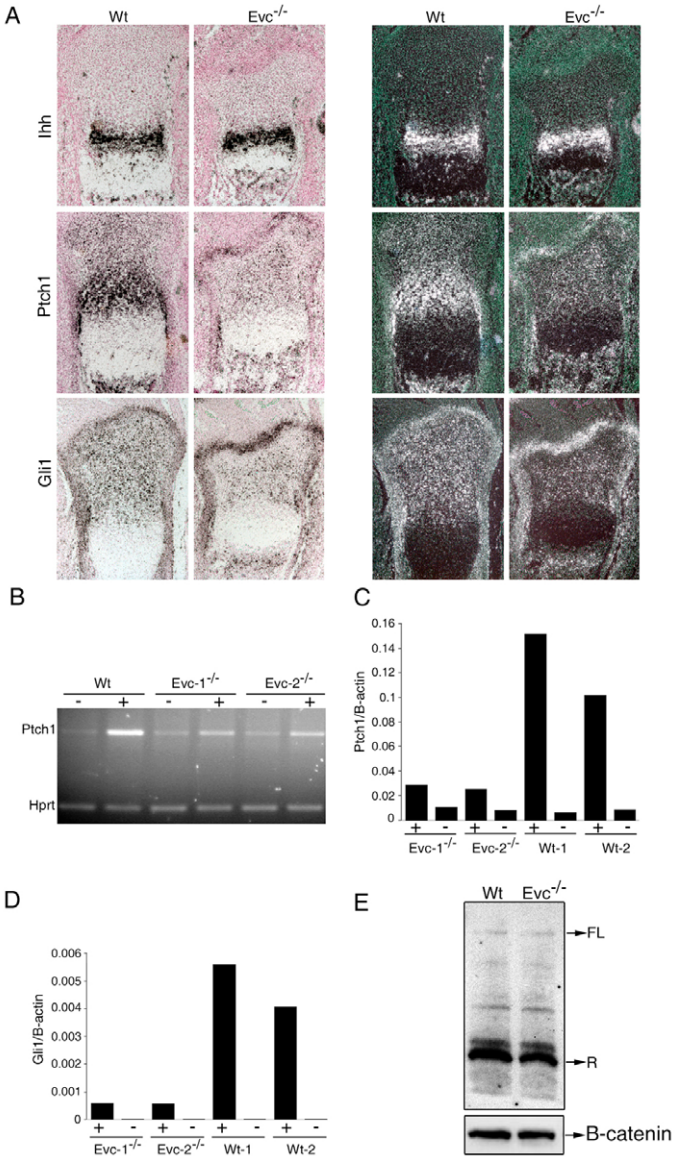

Fig. 6. Evc is required for Ihh signalling. (**A**) Tissue in situ hybridisation analysis from E16.5 embryos showing indistinguishable *Ihh* expression between wild type and mutant, but markedly decreased hybridisation signals of *Ptch1* and *Gli1* in *Evc*$^{-/-}$ embryos. Bright-field (left) and dark-field (right) hybridisation pictures from proximal tibia are shown. (**B**) RT-PCR analysis of *Ptch1* expression in wild-type and two different *Evc*$^{-/-}$ MEF cultures grown with (+) or without (–) purmorphamine. *Hprt* expression is used as a control. (**C**,**D**) *Ptch1*and *Gli1* quantitative RT-PCR analysis in chondrocytes cultured with (+) or without (–) purmorphamine. β-actin was used as control for both quantitative PCR experiments. (**E**) Western blot showing unchanged levels of full-length Gli3 (FL, 190 kDa) and Gli3R (R, 83 kDa) in limb protein extracts of E14.5 wild-type and *Evc*$^{-/-}$ mice. Ratios of the β-catenin control band:Gli3R band were 1.47 and 1.41 for wild-type and *Evc*$^{-/-}$, respectively.

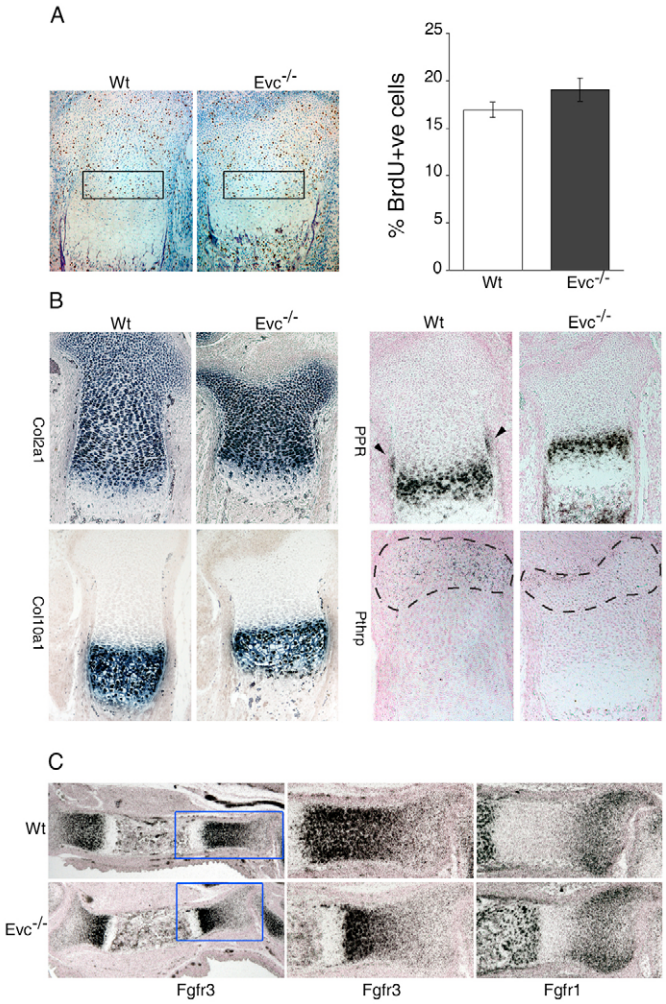

Fig. 7. Evc-deficient mice show premature hypertrophic differentiation of proliferating chondrocytes. (**A**) Analysis of chondrocyte proliferation. On the left, E17.5 wild-type and mutant proximal tibia sections, stained with BrdU immunhistochemistry; the rectangles indicate the areas of columnar chondrocytes that were counted. On the right, bar chart showing that the percentage of BrdU-positive cells in the proliferating zone does not significantly differ between wild type and mutant (ANOVA, P=0.2374). (**B**) Expression of differentiation markers *Col2a1*, *Col10a1*, *Pthrp* and *PPR* in E16.5 wild-type and mutant embryos. The region of *Pthrp* expression is outlined by the dashed line. Note the absence of *PPR* signal in the perichondrium adjacent to late proliferating and early prehypertrophic chondrocytes in *Evc*$^{-/-}$ sections (arrowheads). (**C**) Comparative analysis of *Fgfr3* and *Fgfr1* expression pattern in wild-type and mutant E16.5 distal tibiae. There is no difference in *Fgfr1* expression, but marked shortening of the *Fgfr3* expression domain. The boxed areas of the left-hand panels are shown at high mignification in the middle panels for *Fgfr3* and in the right-hand panels for *Fgfr1*.

Ptch1 expression. Similarly, the bone collar defect is not completely rescued. Lack of function of Gli activators is the likely cause for these features of *Ihh*$^{-/-}$ mice, which are not restored in the double knockouts (Hilton et al., 2005; Koziel et al., 2005). In *Evc*$^{-/-}$ mice, there is low expression of *Gli1*, *Ptch1* and *Pthrp* in the growth plate as observed in the double knockouts. Likewise, both *Evc*$^{-/-}$ mice and the double knockouts have defective bone collar formation as manifest by decreased *PPR* expression in the perichondrium and in the von-Kossa staining. We postulate that *Evc*$^{-/-}$ mice are likely to be deficient in the same Ihh-dependent Gli activator functions that are absent in the *Ihh*$^{-/-}$,*Gli3*$^{-/-}$ mice.

Upregulation of *Ptch1* and *Gli1* expression has previously been observed in cells outlining the cartilage growth plate when *Ptch1* expression is specifically diminished in chondrocytes (Long et al., 2004). The extended range of signalling has been attributed to the absence of Ptch-mediated ligand sequestration (Chen and Struhl, 1996; Lewis et al., 2001). We observed similar expression of *Ptch1* and *Gli1* in the weakly *Evc*-expressing cells surrounding the articular surface in *Evc*$^{-/-}$ mice (Fig. 6A). This indicates that in mice lacking Evc, Hh signalling is most markedly perturbed in those cells that would normally have the highest levels of *Evc* expression.

Bone shortening in *Evc*$^{-/-}$ as a result of premature chondrocyte hypertrophy

Growth plate, and hence bone, shortening could result from one or more of the following: decreased proliferation, increased apoptosis, premature differentiation either of distal to columnar chondrocyte or from proliferating to hypertrophic chondrocytes. In *Evc*$^{-/-}$ mice, proliferation appears normal, consistent with the normal Gli3R levels observed in western blotting, and apoptosis also appears normal. Differentiation from distal to columnar chondrocyte, which is regulated by Gli3R levels (Koziel et al., 2005), is also normal in *Evc*$^{-/-}$ mice. As shown by the considerable reduction in size of the *Fgfr3* expression domain, the *Evc*$^{-/-}$ growth plate shortening is explained by the shorter region of proliferating columns of chondrocytes, which in turn is due to the premature onset of hypertrophic differentiation. Hypertrophic differentiation is regulated by Pthrp, itself a target of Gli activation (Koziel et al., 2005). Thus, we can conclude that premature hypertrophic differentiation in *Evc*$^{-/-}$ chondrocytes is due to decreased *Pthrp* expression secondary to defective Hh signalling.

Comparison of *Evc*$^{-/-}$ with IFT mutants

Defects in IFT cause embryonic lethality and it is only with the advent of mice carrying a conditional *Ift88* allele and the *Prx1Cre* transgene that it has been possible to study endochondral bone formation in IFT mutants (Haycraft et al., 2007). *Evc*$^{-/-}$ and the *Prx1Cre Ift88* conditional mice both have decreased activation of Ihh targets *Ptch1* and *Gli1* in the growth plates of long bones and delayed bone collar formation, features that are not fully rescued by Gli3R derepression in the *Ihh*$^{-/-}$,*Gli3*$^{-/-}$ mice and that are expected to be associated with defective Gli activation. *Evc* mutants differ from the IFT conditionals with respect to Gli3R, which is decreased in the IFT nulls. Chondrogenic clumps of cells surrounding the perichondrium are described in *Prx1Cre Ift88* conditional mice, a feature that we have not observed in the *Evc* mutant and not reported in the *Ihh*$^{-/-}$,*Gli3*$^{-/-}$ mice. An additional difference between IFT and *Evc* mutants relates to *Ihh* expression, which appears normal in *Evc*$^{-/-}$ mice but is reduced in the *Prx1Cre* conditional allele of *Ift88*.

Evc involvement in Shh signalling

Evc-depleted mice phenocopy most of the EvC features and therefore represent a good model for this syndrome. They reproduce the skeletal and dental anomalies of the condition and the perinatal lethality. Similar neonatal losses in *Ihh*$^{-/-}$ and *Pthrp*$^{-/-}$ mice have been attributed to respiratory failure secondary to the small rib cage (Karaplis et al., 1998; St-Jacques et al., 1999). The lack of polydactyly in *Evc*$^{-/-}$ mice came as a surprise as EvC individuals

invariably have postaxial polydactyly of the hands. Neither *Gli1* nor *Gli2* mutant mice manifest limb patterning defects (Park et al., 2000). However, the spontaneous and targeted *Gli3* mutants have polydactyly, and polydactyly also occurs in human disorders caused by *Gli3* mutations such Pallister-Hall syndrome and Greig cephalopolysyndactyly syndrome (Ehlen et al., 2006). In many of the mutants with polydactyly, including the IFT mutants, both Gli3 activator function and Gli3 repression are perturbed. It is apparent that the balance between Gli3 activation and Gli3 repression across the limb bud is crucial in specifying the number of digits (Ahn and Joyner, 2004; Wang et al., 2007). The fact that we did not detect *lacZ* expression in the limb buds of $Evc^{-/-}$ mice when patterning is being established indicates that *Evc* expression in the limb buds is low compared with that in bone anlagen, and this might explain the absence of polydactyly in $Evc^{-/-}$ mice. Regardless, as anteroposterior patterning in the limb bud is regulated by Shh rather than Ihh, the polydactyly seen in EvC individuals suggests that *EVC* may also play a crucial role in transduction of Shh signalling during human limb bud morphogenesis. The occasional observation of a single central incisor in $Evc^{-/-}$ mice is also suggestive of defective Shh signalling in the mouse given that this is a feature seen in association with holoprosencephaly due to *SHH* mutations. Similarly, temperospatial expression of *lacZ* in tissues where Shh is expressed, such as the orofacial region and vibrissae (Bitgood and McMahon, 1995), is consistent with *Evc* participation in the transduction of the Shh signal.

Conclusion

We have shown that Evc localises at the distal end of the basal body and the base of the axoneme and that it is integral to Ihh signalling in developing bones. Intracellular transduction of Hh signal is not yet fully understood. There have been surprises – knockdowns of two of the components of the pathway first identified in *Drosophila*, Sufu and Fu, indicate that their roles differ between *Drosophila* and vertebrates (Svard et al., 2006; Varjosalo et al., 2006). Evc adds to the differences between *Drosophila* and vertebrates, as there are no recognisable Evc homologues in organisms other than vertebrates. In the last few years, new players have been identified acting downstream of Smo in mice [Rab23 (Eggenschwiler et al., 2006) and tectonic (Reiter and Skarnes, 2006)], in zebrafish [Iguana (also known as Dzip1 – ZFIN) (Sekimizu et al., 2004; Wolff et al., 2004)] and in chick [Talpid (Davey et al., 2006)], the precise role of which remain to be elucidated. Here we show that Evc is a novel basal body component of Hh signalling indispensable for normal endochondral growth, acting downstream of Smo to facilitate transcription of the Ihh-regulated genes.

We thank Paul Cairns and Weiping Li for help with blastocyst injections and embryo transfers; Dr Ralf Kist for the vectors used in the construction of the targeting vector; Dr Erik E. Turner for plasmid pSDKpA; Dr Andreas Schedl for the AB1 ES cells; Dr Fanxin Long, Dr Matthew Hilton and Dr Andrew McMahon for the *Ihh*, *Ptch1* and *Pthrp* probes; Dr Bjorn Olsen for *Col2a1* and *Col10a1* probes; Dr Andrea Vortkamp for *Fgfr1*, *Fgfr3* probes; and Dr Baolin Wang for the Gli3 antibody. This work was supported by the MRC, Spanish Ministerio de Educacion y Ciencia, BBSRC, BHF and the Nuffield Foundation's Oliver Bird Rheumatism Programme. V.L.R.-P. acknowledges Dr Santiago Rodriguez de Córdoba for support.

Supplementary material

Supplementary material for this article is available at
http://dev.biologists.org/cgi/content/full/134/16/2903/DC1

References

Ahn, S. and Joyner, A. (2004). Dynamic changes in the response of cells to positive hedgehog signaling during mouse limb patterning. *Cell* **118**, 505-516.
Bitgood, M. and McMahon, A. (1995). Hedgehog and Bmp genes are coexpressed at many diverse sites of cell-cell interaction in the mouse embryo. *Dev. Biol.* **172**, 126-138.
Chen, Y. and Struhl, G. (1996). Dual roles for patched in sequestering and transducing Hedgehog. *Cell* **87**, 553-563.
Chung, U.-i., Lanske, B., Lee, K., Li, E. and Kronenberg, H. (1998). The parathyroid hormone/parathyroid hormone-related peptide receptor coordinates endochondral bone development by directly controlling chondrocyte differentiation. *Proc. Natl. Acad. Sci. USA* **95**, 13030-13035.
Corbit, K., Aanstad, P., Singla, V., Norman, A., Stainier, D. and Reiter, J. (2005). Vertebrate Smoothened functions at the primary cilium. *Nature* **437**, 1018-1021.
Davey, M. G., Paton, I. R., Yin, Y., Schmidt, M., Bangs, F. K., Morrice, D. R., Smith, T. G., Buxton, P., Stamataki, D., Tanaka, M. et al. (2006). The chicken talpid3 gene encodes a novel protein essential for Hedgehog signaling. *Genes Dev.* **20**, 1365-1377.
Eggenschwiler, J., Bulgakov, O., Qin, J., Li, T. and Anderson, K. (2006). Mouse Rab23 regulates hedgehog signaling from smoothened to Gli proteins. *Dev. Biol.* **290**, 1-12.
Ehlen, H., Buelens, L. and Vortkamp, A. (2006). Hedgehog signaling in skeletal development. *Birth Defects Res. C Embryo Today* **78**, 267-279.
Haycraft, C., Banizs, B., Aydin-Son, Y., Zhang, Q., Michaud, E. and Yoder, B. (2005). Gli2 and Gli3 localize to cilia and require the intraflagellar transport protein polaris for processing and function. *PLoS Genet.* **1**, e53.
Haycraft, C., Zhang, Q., Song, B., Jackson, W., Detloff, P., Serra, R. and Yoder, B. (2007). Intraflagellar transport is essential for endochondral bone formation. *Development* **134**, 307-316.
Hilton, M., Tu, X., Cook, J., Hu, H. and Long, F. (2005). Ihh controls cartilage development by antagonizing Gli3, but requires additional effectors to regulate osteoblast and vascular development. *Development* **132**, 4339-4351.
Hogan, B., Beddington, R., Constantini, F. and Lacy, E. (1994). Staining for β-galactosidase (lacZ) activity. In *Manipulating the Mouse Embryo* (ed. B. Hogan, R. Beddington, F. Constantini and E. Lacy), pp. 373-375. Cold Spring Harbor, NY: Cold Spring Harbor Laboratory Press.
Hooper, J. and Scott, M. (2005). Communicating with Hedgehogs. *Nat. Rev. Mol. Cell Biol.* **6**, 306-317.
Huangfu, D. and Anderson, K. (2005). Cilia and Hedgehog responsiveness in the mouse. *Proc. Natl. Acad. Sci. USA* **102**, 11325-11330.
Huangfu, D., Liu, A., Rakeman, A., Murcia, N., Niswander, L. and Anderson, K. (2003). Hedgehog signalling in the mouse requires intraflagellar transport proteins. *Nature* **426**, 83-87.
Karaplis, A., He, B., Nguyen, M., Young, I., Semeraro, D., Ozawa, H. and Amizuka, N. (1998). Inactivating mutation in the human parathyroid hormone receptor type 1 gene in Blomstrand chondrodysplasia. *Endocrinology* **139**, 5255-5258.
Kessel, M. and Gruss, P. (1991). Homeotic transformations of murine vertebrae and concomitant alteration of Hox codes induced by retinoic acid. *Cell* **67**, 89-104.
Koziel, L., Wuelling, M., Schneider, S. and Vortkamp, A. (2005). Gli3 acts as a repressor downstream of Ihh in regulating two distinct steps of chondrocyte differentiation. *Development* **132**, 5249-5260.
Kronenberg, H. (2003). Developmental regulation of the growth plate. *Nature* **423**, 332-336.
Lanske, B., Karaplis, A., Lee, K., Luz, A., Vortkamp, A., Pirro, A., Karperien, M., Defize, L., Ho, C., Mulligan, R. et al. (1996). PTH/PTHrP receptor in early development and Indian hedgehog-regulated bone growth. *Science* **273**, 663-666.
Lescher, B., Haenig, B. and Kispert, A. (1998). sFRP-2 is a target of the Wnt-4 signaling pathway in the developing metanephric kidney. *Dev. Dyn.* **213**, 440-451.
Lewis, P. M., Dunn, M. P., McMahon, J. A., Logan, M., Martin, J. F., St-Jacques, B. and McMahon, A. P. (2001). Cholesterol modification of sonic hedgehog is required for long-range signaling activity and effective modulation of signaling by Ptc1. *Cell* **105**, 599-612.
Liu, A., Wang, B. and Niswander, L. (2005). Mouse intraflagellar transport proteins regulate both the activator and repressor functions of Gli transcription factors. *Development* **132**, 3103-3111.
Long, F., Chung, U.-i., Ohba, S., McMahon, J., Kronenberg, H. M. and McMahon, A. P. (2004). Ihh signaling is directly required for the osteoblast lineage in the endochondral skeleton. *Development* **131**, 1309-1318.
May, S., Ashique, A., Karlen, M., Wang, B., Shen, Y., Zarbalis, K., Reiter, J., Ericson, J. and Peterson, A. (2005). Loss of the retrograde motor for IFT disrupts localization of Smo to cilia and prevents the expression of both activator and repressor functions of Gli. *Dev. Biol.* **287**, 378-389.
McKusick, V., Egeland, J., Eldridge, R. and Krusen, D. (1964). Dwarfism in the Amish I. The Ellis-van Creveld syndrome. *Bull. Johns Hopkins Hosp.* **115**, 306-336.
Naski, M., Colvin, J., Coffin, J. and Ornitz, D. (1998). Repression of hedgehog signaling and BMP4 expression in growth plate cartilage by fibroblast growth factor receptor 3. *Development* **125**, 4977-4988.
Park, H., Bai, C., Platt, K., Matise, M., Beeghly, A., Hui, C., Nakashima, M.

and Joyner, A. (2000). Mouse Gli1 mutants are viable but have defects in SHH signaling in combination with a Gli2 mutation. *Development* **127**, 1593-1605.
Razzaque, M., Soegiarto, D., Chang, D., Long, F. and Lanske, B. (2005). Conditional deletion of Indian hedgehog from collagen type 2alpha1-expressing cells results in abnormal endochondral bone formation. *J. Pathol.* **207**, 453-461.
Reiter, J. and Skarnes, W. (2006). Tectonic, a novel regulator of the Hedgehog pathway required for both activation and inhibition. *Genes Dev.* **20**, 22-27.
Ruiz-Perez, V. L., Ide, S., Strom, T., Lorenz, B., Wilson, D., Woods, K., King, L., Francomano, C., Freisinger, P., Spranger, S. et al. (2000). Mutations in a new gene in Ellis-van Creveld syndrome and Weyers acrodental dysostosis. *Nat. Genet.* **24**, 283-286.
Ruiz-Perez, V. L., Tompson, S., Blair, H., Espinoza-Valdez, C., Lapunzina, P., Silva, E., Hamel, B., Gibbs, J., Young, I., Wright, M. et al. (2003). Mutations in two nonhomologous genes in a head-to-head configuration cause Ellis-van Creveld syndrome. *Am. J. Hum. Genet.* **72**, 728-732.
Schatz, O., Golenser, E. and Ben-Arie, N. (2005). Clearing and photography of whole mount X-gal stained mouse embryos. *BioTechniques* **39**, 650-656.
Sekimizu, K., Nishioka, N., Sasaki, H., Takeda, H., Karlstrom, R. and Kawakami, A. (2004). The zebrafish iguana locus encodes Dzip1, a novel zinc-finger protein required for proper regulation of Hedgehog signaling. *Development* **131**, 2521-2532.
Shingleton, W. D., Ellis, A. J., Rowan, A. D. and Cawston, T. E. (2000). Retinoic acid combines with interleukin-1 to promote the degradation of collagen from bovine nasal cartilage: matrix metalloproteinases-1 and -13 are involved in cartilage collagen breakdown. *J. Cell. Biochem.* **79**, 519-531.
Sinha, S. and Chen, J. (2006). Purmorphamine activates the Hedgehog pathway by targeting Smoothened. *Nat. Chem. Biol.* **2**, 29-30.
St-Jacques, B., Hammerschmidt, M. and McMahon, A. (1999). Indian hedgehog signaling regulates proliferation and differentiation of chondrocytes and is essential for bone formation. *Genes Dev.* **13**, 2072-2086.
Svard, J., Heby-Henricson, K., Persson-Lek, M., Rozell, B., Lauth, M., Bergstrom, A., Ericson, J., Toftgard, R. and Teglund, S. (2006). Genetic elimination of Suppressor of fused reveals an essential repressor function in the mammalian Hedgehog signaling pathway. *Dev. Cell* **10**, 187-197.
Todaro, G. and Green, H. (1963). Quantitative studies of the growth of mouse embryo cells in culture and their development into established lines. *J. Cell Biol.* **17**, 299-313.
Tompson, S., Ruiz-Perez, V. L., Blair, H., Barton, S., Navarro, V., Robson, J., Wright, M. and Goodship, J. (2007). Sequencing EVC and EVC2 identifies mutations in two-thirds of Ellis-van Creveld syndrome patients. *Hum. Genet.* **120**, 663-670.
Varjosalo, M., Li, S. and Taipale, J. (2006). Divergence of hedgehog signal transduction mechanism between Drosophila and mammals. *Dev. Cell* **10**, 177-186.
Vortkamp, A., Lee, K., Lanske, B., Segre, G. V., Kronenberg, H. M. and Tabin, C. (1996). Regulation of rate of cartilage differentiation by Indian hedgehog and PTH-related protein. *Science* **273**, 613-622.
Wang, C., Pan, Y. and Wang, B. (2007). A hypermorphic mouse Gli3 allele results in a polydactylous limb phenotype. *Dev. Dyn.* **236**, 769-776.
Weir, E., Philbrick, W., Amling, M., Neff, L., Baron, R. and Broadus, A. (1996). Targeted overexpression of parathyroid hormone-related peptide in chondrocytes causes chondrodysplasia and delayed endochondral bone formation. *Proc. Natl. Acad. Sci. USA* **93**, 10240-10245.
Wolff, C., Roy, S., Lewis, K., Schauerte, H., Joerg-Rauch, G., Kirn, A., Weiler, C., Geisler, R., Haffter, P. and Ingham, P. (2004). iguana encodes a novel zinc-finger protein with coiled-coil domains essential for Hedgehog signal transduction in the zebrafish embryo. *Genes Dev.* **18**, 1565-1576.
Wu, X., Walker, J., Zhang, J., Ding, S. and Schultz, P. (2004). Purmorphamine induces osteogenesis by activation of the hedgehog signaling pathway. *Chem. Biol.* **11**, 1229-1238.